

ORIGINAL ARTICLE

Abnormal Development of Neural Stem Cell Niche in the Dentate Gyrus of Menkes Disease

Sung-kuk Cho¹, Suhyun Gwon¹, Hyun Ah Kim¹, Jiwon Kim², Sung Yoo Cho¹, Dong-Eog Kim², Jong-Hee Chae³, Dae Hwi Park^{1,*}, Yu Kyeong Hwang^{1,*}

¹Cell Therapy Research Center, GC Cell, Yongin, Korea

²Department of Neurology, Dongguk University Ilsan Hospital, Goyang, Korea

³Department of Pediatrics, Seoul National University Children's Hospital, Seoul National University College of Medicine, Seoul, Korea

Background and Objectives: Menkes disease (MNK) is a rare X-linked recessive disease, caused by mutations in the copper transporting ATP7A gene that is required for copper homeostasis. MNK patients experience various clinical symptoms including neurological defects that are closely related to the prognosis of MNK patients. Neural stem cells (NSCs) in the hippocampal dentate gyrus (DG) produce new neurons throughout life, and defects in DG neurogenesis are often correlated with cognitive and behavioral problems. However, neurodevelopmental defects in the DG during postnatal period in MNK have not been understood yet.

Methods and Results: Mottled-brindled ($Mo^{Br/y}$) mice (MNK mice) and littermate controls were used in this study. *In vivo* microCT imaging and immunohistochemistry results demonstrate that blood vasculatures in hippocampus are abnormally decreased in MNK mice. Furthermore, postnatal establishment of NSC population and their neurogenesis are severely compromised in the DG of MNK mice. In addition, *in vitro* analyses using hippocampal neurosphere culture followed by immunocytochemistry and immunoblotting suggest that neurogenesis from MNK NSCs is also significantly compromised, corresponding to defective neurogenic gene expression in MNK derived neurons.

Conclusions: Our study is the first reports demonstrating that improper expansion of the postnatal NSC population followed by significant reduction of neurogenesis may contribute to neurodevelopmental symptoms in MNK. In conclusion, our results provide new insight into early neurodevelopmental defects in MNK and emphasize the needs for early diagnosis and new therapeutic strategies in the postnatal central nerve system damage of MNK patients.

Keywords: Menkes disease, ATP7A, Vascularization, Hippocampus, Neural stem cell, Neurogenesis

Received: May 5, 2021, Revised: December 16, 2021, Accepted: December 19, 2021, Published online: February 28, 2022

Correspondence to **Dae Hwi Park**

Cell Therapy Research Center, GC Cell, 107, Ihyeon-ro 30beon-gil, Giheung-gu, Yongin 16924, Korea

Tel: +82-31-260-0822, Fax: +82-31-260-1800, E-mail: parkdh@gccorp.com

Co-Correspondence to **Yu Kyeong Hwang**

Cell Therapy Research Center, GC Cell, 107, Ihyeon-ro 30beon-gil, Giheung-gu, Yongin 16924, Korea

Tel: +82-31-260-9853, Fax: +82-31-260-9870, E-mail: ykhwang@gccorp.com

*These authors contributed equally to this work.

© This is an open-access article distributed under the terms of the Creative Commons Attribution Non-Commercial License (<http://creativecommons.org/licenses/by-nc/4.0/>), which permits unrestricted non-commercial use, distribution, and reproduction in any medium, provided the original work is properly cited.

Copyright © 2022 by the Korean Society for Stem Cell Research

Introduction

Menkes disease (MNK) is a rare X-linked recessive disorder, caused by mutations in the copper transporting ATP7A gene, which may lead to disruption of copper homeostasis in the body (1-4). Since ATP7A is abundantly expressed in the placenta, lung, kidney, testis, and brain (5), MNK patients have a variety of clinical symptoms such as kinky hair, growth failure, and abnormal brain development. In particular, neurological defects such as hypotonia, lethargic states, seizures, and vascular and cerebral atrophy are closely related to the survival of patients who usually do not live past the age 3 years (4). Therefore, understanding the effects of ATP7A mutations during brain development may provide critical insights into how ATP7A dysfunction can underlie neurodevelopmental defects in MNK patients.

Copper is abundant in basal ganglia, hippocampus, and cerebellum in the brain (6) and is required as a cofactor for Cu/Zn superoxide dismutase (SOD), peptidyl α -amidating monooxygenase (PAM), dopamine β -hydroxylase, cytochrome C oxidase, and ceruloplasmin (7). ATP7A dysfunction in the brain may cause accumulation of copper in endothelial cells located in the blood brain barrier, which eventually leads to insufficient copper supply to neighboring neurons and glial cells. The insufficient supply of copper has been reported to result in gradual neurodegenerative damage or interruption of central nervous system (CNS) development (8). Several studies suggest that dysfunctional cerebellar Purkinje cells may be one of the major contributors to MNK (9, 10). However, effects of ATP7A dysfunction in other brain regions during postnatal development still have not been fully demonstrated.

Hippocampus plays a crucial role in certain forms of learning, memory, and emotional behavior in the brain (11, 12). In the adult hippocampus, neural stem cells (NSCs) that reside in subgranular zone (SGZ) of the dentate gyrus (DG) generate granule neurons throughout life. Defective hippocampal formation has been reported in several congenital disorders such as holoprosencephaly, polymicrogyria, lissencephaly, and in children with epilepsy (13). Furthermore, abnormal DG neurogenesis has been associated with cognitive defects including autism spectrum disorders (14, 15). However, congenital DG abnormalities in MNK have not been elucidated. In this study, we demonstrated abnormal postnatal NSC niche development followed by severe neurogenesis defects in DG after birth using MNK mice model. Our results provide new insights into understanding defects in postnatal brain

development in MNK that may underlie cognitive and neurological impairment in MNK patients.

Materials and Methods

Animals

A colony of mottled-brindled ($Mo^{Br/y}$) mice (16) was maintained by mating an adult female heterozygous mottled brindled (C57BL/6J $Mo^{Br/+}$) mouse with a wild type male C57BL/6J mice (Jackson Laboratory; Bar Harbor, ME). Mice were bred and maintained on a 12 h light, 12 h dark cycle in the animal care facility at the Green Cross R&D center, Yongin, Korea. All the animal protocols were approved by the Green Cross Animal Care and Use Committee prior to experiments. In this study, both male (+/y) and female (+/+) littermates were used as controls. Early postnatal animals were euthanized by decapitation after being anesthetized on ice.

In vivo microCT imaging

Briefly, postnatal day 14 mice were anesthetized using isoflurane (JW Pharmaceutical Co., Seoul, South Korea) via nose cone (1.0~1.5% mixed with 1~2 L/min O_2) and blood was removed through heart perfusion with cold PBS (1 ml). Microfil reagent[®] (Flow Tech, Inc., Carver, MA) for microvessel siliconization was prepared with Compound : Diluent : Hardener=45 : 50 : 5 ratio (by weight) and immediately injected into the heart using 1 ml syringe. 90 minute after injection, brains were imaged with a microCT small animal imager (NFR Polaris-G90; NanoFocusRay, Jeonju, Korea).

Rhodanine stain

Rhodanine stain was prepared as previously described (17). Briefly, 0.1% Rhodanine stock solution was prepared by adding 0.1 g of 5-(p-dimethylaminobenzylidene) Rhodanine (Sigma-Aldrich, St. Louis, MO) in 100 ml ethanol. Brain sections were incubated with Rhodanine working solution (Stock solution : deionized water=4 : 6) at 60°C for 60 min. Rhodanine stained sections were washed four times with deionized water and counterstained with methylene blue (Sigma-Aldrich, St. Louis, MO). Then, Rhodamine stained sections were rinsed in 0.5% sodium borate solution and three times in deionized water. Stained section was dehydrated with ethanol and xylene and mounted with a cover glass using Permount solution (Thermo, South Logan, UT).

Cell culture

Primary neurosphere culture was established as previously described (18). Briefly, hippocampal tissue was micro-dissected from E18.5 embryos and incubated with Accutase solution (Innovative Cell Technologies, San Diego, CA) with 0.02% DNase I (Roche, Indianapolis, IN) for 15 min at 37°C. After incubation, the tissue was rinsed with Mg²⁺ and Ca²⁺ free HBSS (Gibco-Invitrogen, Grand Island, NY) and resuspended with 2 ml culture medium. Hippocampal cells were dissociated by gentle pipetting and plated at 1×10⁴ cells/ml into a 10 mm petri dish and incubated at 37°C with 5% CO₂. Neurosphere culture was performed with culture medium composed of DMEM/F12 (1 : 1) supplemented with N2 (Gibco-Invitrogen, Grand Island, NY), 20 ng/ml EGF (Sigma-Aldrich, St. Louis, MO), 20 ng/ml bFGF (Dong-A Pharmaceutical Co., Yongin, South Korea), 5 mM HEPES (Sigma-Aldrich, St. Louis, MO), 25 mg/ml gentamicin, and penicillin/streptomycin (100 U/ml) (Gibco-Invitrogen, Grand Island, NY). Culture medium was exchanged every 2 days. To examine neurosphere differentiation efficiency, neurospheres were plated on coverslips coated with 0.1 mg/ml poly-L-lysine (Sigma-Aldrich, St. Louis, MO) in MEM (Gibco BRL, Gaithersburg, MD), supplemented with 10% FBS (HyClone, South Logan, UT), 0.45% glucose, 1 mM sodium pyruvate, 2 mM glutamine and 50 mg/ml gentamicin for 4 hours. To induce neuronal differentiation, the medium was replaced with serum-free Neurobasal medium (Gibco BRL, Gaithersburg, MD) supplemented with B27 (Gibco BRL, Gaithersburg, MD), Glutamax (Gibco-Invitrogen, Grand Island, NY), and 200 nM cytosine arabinoside (Sigma-Aldrich, St. Louis, MO). For copper accumulation assay, copper (1 μg/ml) was added into the culture medium along with copper chloride (1 μg/μL, Sigma-Aldrich, St. Louis, MO) as previously described (19, 20).

Immunohistochemistry

Brains were fixed by intracardiac perfusion with 0.1 N phosphate buffer containing 4% paraformaldehyde (Sigma-Aldrich, St. Louis, MO) as previously described (21). Before immunohistochemistry, heat-induced antigen retrieval was performed with 0.01 M sodium citrate (pH 6.0) for 20 min (21). For immunohistochemistry, 12 μm frozen sections were immunostained with the following primary antibodies : anti-Nestin (1 : 200; Millipore, Billerica, MA); anti-SOX2 (1 : 200; Rabbit, Cell Signaling Technology, Inc., Beverly, MA); anti-SOX2 (1 : 200; Mouse, BD Biosciences Pharmingen, San Diego, CA); anti-GLUT1 (1 : 200; Millipore, Billerica, MA); anti-DCX

(1 : 200; Millipore, Billerica, MA); anti-PROX1 (1 : 200; BioLegend, San Diego, CA); anti-MAP2 (1 : 200; Cell Signaling Technology, Inc., Beverly, MA); anti-GFAP (1 : 200; Cell Signaling Technology, Inc., Beverly, MA); anti-NeuN (1 : 200; Millipore, Billerica, MA); anti-Calbindin (1 : 200; Cell Signaling Technology, Inc., Beverly, MA); anti-Ki67 (1 : 200; Cell Signaling Technology, Inc., Beverly, MA); anti-Cleaved Caspase 3 (1 : 200; Cell Signaling Technology, Inc., Beverly, MA). Sections were blocked with PBS containing 10% normal goat serum and 0.1% bovine albumin serum, before primary antibody incubation at 4°C overnight. Goat Alexa Fluor 488 and 594 conjugated secondary antibodies (1 : 500; Invitrogen, Carlsbad, CA) and 1 μg/ml DAPI (Sigma-Aldrich, St. Louis, MO) for nuclear counterstaining were also used. Microscopic images were acquired with a LSM710 confocal microscope (Carl Zeiss, Oberkochen, Germany).

Immunocytochemistry

Cells were fixed with ice-cold methanol at -20°C for 20 min. After washing with PBS, fixed cells were incubated with blocking solution (10% normal goat serum, 0.1% bovine serum albumin, and 0.1% Triton X-100 in PBS) for 1 h at room temperature. An anti-MAP2 (1 : 200; Cell Signaling Technology, Inc., Beverly, MA) and anti-GFAP antibody (1 : 200; Cell Signaling Technology, Inc., Beverly, MA) were incubated with fixed cells overnight at 4°C. After washing, fixed cells were further incubated with Goat Alexa Fluor 488 and 594 conjugated secondary antibodies (1 : 500; Gibco-Invitrogen, Grand Island, NY) and 1 μg/ml DAPI (Sigma-Aldrich, St. Louis, MO) for nuclear counterstaining.

Immunoblotting

Cells were lysed in ice-cold RIPA containing cOmplete[®] Protease Inhibitor Cocktail Tablets (Roche, Indianapolis, IN) for 30 min, followed by centrifugation at 12,000 rpm for 15 min at 4°C for collecting cell lysate. Standard gel electrophoresis was performed and proteins were transferred onto a PVDF membrane (Schleicher & Schuell, Keene, NH). Following primary and secondary antibodies were used for immunoblotting; anti-pAKT (1 : 500; Ser473, Cell Signaling Technology, Beverly, MA); anti-AKT (1 : 500; Cell Signaling Technology, Inc., Beverly, MA); anti-pERK (1 : 500; Thr202/Tyr204, Cell Signaling Technology, Inc., Beverly, MA); anti-ERK1/2 (1 : 500; Cell Signaling Technology, Inc., Beverly, MA); anti-pSTAT3 (1 : 500; Thr183/Tyr185, Cell Signaling Technology, Inc., Beverly, MA); anti-STAT3 (1 : 500; Cell

Signaling Technology, Inc., Beverly, MA); anti-NeuroD (1 : 500; Chemicon, Temecula, CA); anti-JAK2 (1 : 500; Millipore, Billerica, MA); anti- β actin (1 : 1000, Sigma-Aldrich, St. Louis, MO); HRP-conjugated secondary antibodies (1 : 2000; Thermo, South Logan, UT). Protein

bands were imaged with SuperSignal West Pico Chemiluminescent Substrate (Pierce, Rockford, IL).

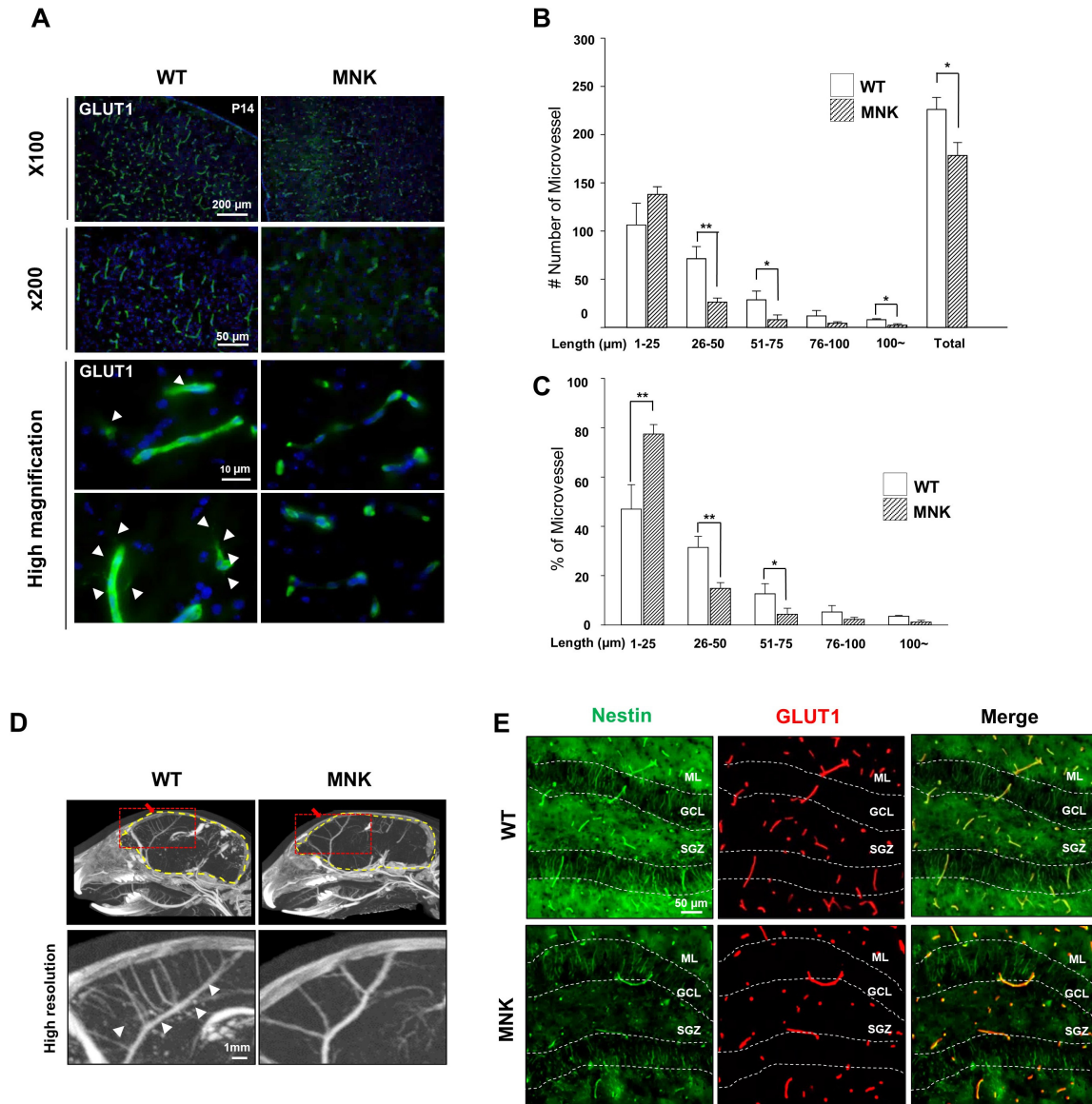


Fig. 1. Abnormal blood vessel development in P14 cerebral cortex and hippocampal dentate gyrus of MNK mice. (A) GLUT1 (marker of brain microvessel) was used to analyze brain vessel pattern in cerebral cortex of wild type and MNK mice. Expression of GLUT1 was decreased in P14 cerebral cortex of MNK mice compared with that of wild type. Scale bar 100 μm (upper), 50 μm (lower). Arrowheads in high magnification image show that sprouting formation in neovascular endothelial tip was reduced in P14 cerebral cortex of MNK mouse. DAPI was used to counterstain nuclei (Blue). (B, C) Quantitative data of blood vessels length show that number and proportion of blood vessels less than 25 μm length was increased in the P13 MNK cerebral cortex. * $p < 0.05$, ** $p < 0.01$ by t-test. (D) Reduction of brain vessels revealed by microCT scan indicates the defect of cerebral vascular structure in the P14 of MNK mice. The red box indicates regions shown in below. (E) P13 hippocampal dentate gyrus of MNK mice were stained with neural stem cell marker NESTIN and cerebral vessel marker GLUT1. Decreased NESTIN⁺ radial processes and blood vessels in the P13 hippocampal dentate gyrus of MNK mice were observed compared to wild type littermate. Scale bar 50 μm . SGZ, subgranular zone; GCL, granule cell layer; ML, molecular layer.

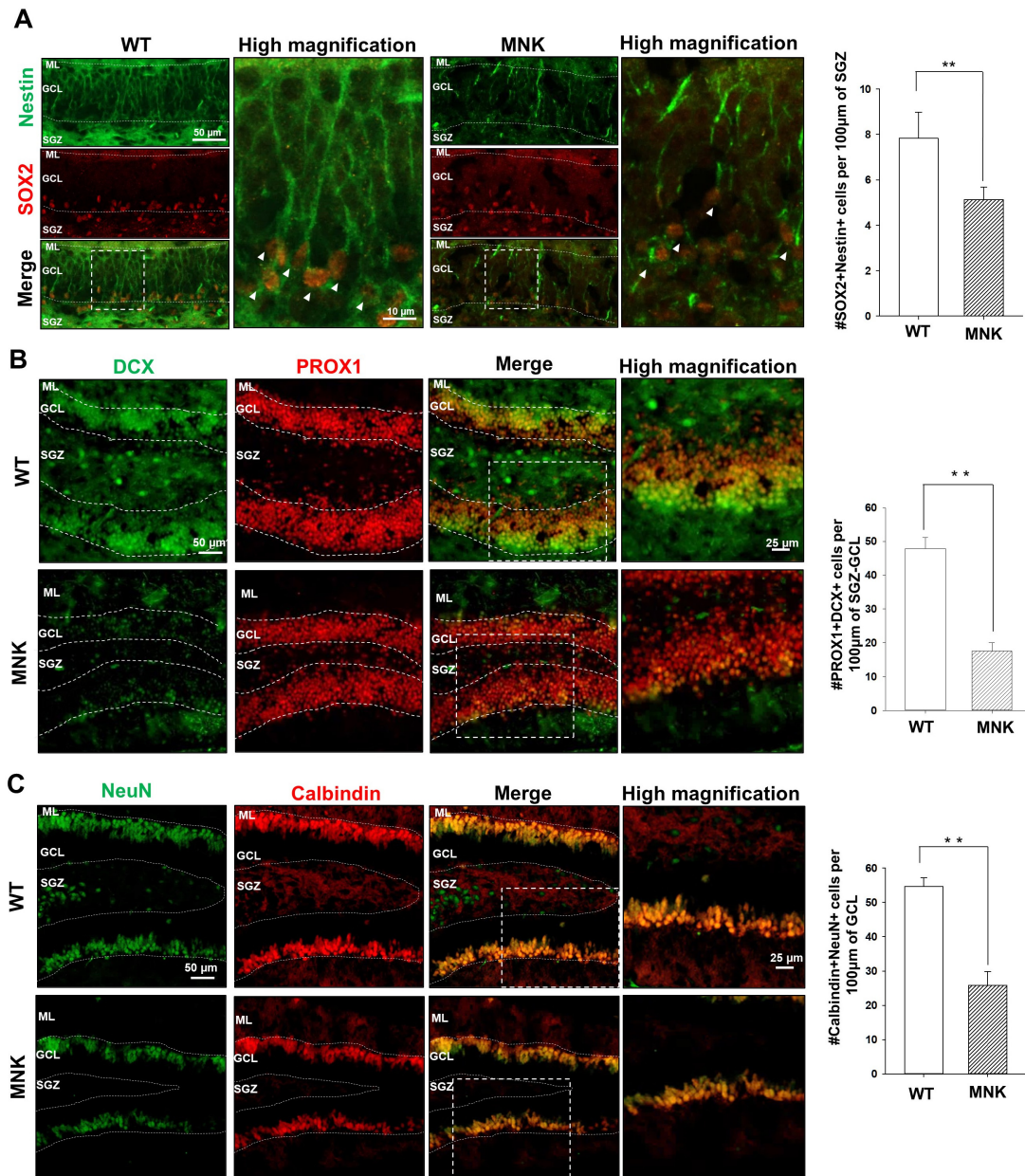


Fig. 2. Neural stem cells and neural progenitors are severely compromised in the dentate gyrus of MNK mice. (A) NESTIN and SOX2 immunostainings were used to identify neural stem cells in the brain of P13 wild type and MNK mice. Neural stem cells in the dentate gyrus were significantly reduced in the brain of P13 MNK mice compared with wild type. White arrowheads of high magnification image indicate neural stem cells stained by NESTIN or SOX2 respectively. Number of NESTIN+, SOX2+ NSCs per 100 μm of SGZ were significantly reduced in the MNK mice compared to control. Scale bar 50 μm and 10 μm (high magnification). (B) Coronal sections of P13 mouse brains were stained with neural progenitor cell marker doublecortin (DCX, Green) and Prospero homeobox protein 1 (PROX1, Red). DCX+ and PROX1+ neural progenitor cells were reduced respectively in GCL. Furthermore, number of DCX+, PROX1+ cells were also significantly reduced by 63% per 100 μm of the GCL and SGZ of MNK mice compared to control. **p<0.001, n=4 each, by t-test. (C) Coronal sections of P13 mouse brains were stained with neuronal marker NeuN and mature neuron maker Calbindin. Number of NeuN+, Calbindin+ mature neurons were significantly decreased by 55% in MNK mice compared with wild type per 100 μm of the upper GCL region of the dentate gyrus. The White box indicates regions shown in high magnification. Scale bar 50 μm. SGZ, subgranular zone; GCL, granule cell layer; ML, molecular layer. *p<0.05, n=4 each, by t-test. **p<0.001, n=4 each, by t-test.

Results

Abnormal copper accumulation in the central nervous system of MNK mice

Copper is accumulated in astrocytes and endothelial cells of blood brain barrier (BBB) in the MNK disease (22). To confirm the copper accumulation in the brain of MNK mice, we carried out Rhodanine staining with brain sections of MNK mice at postnatal day 14 (P14) because new born MNK mice usually cannot live longer than 2 weeks. Rhodanine staining showed large accumulation of bivalent cations in P14 MNK cerebral cortex compared with that of wild type (Supplementary Fig. S1A). Neurons generally receive copper from astrocytes and endothelial cells, but MNK neurons cannot obtain copper from them due to mutation of copper transporter ATP7A gene (8, 23). In order to measure copper transfer capability of MNK neurons and astrocytes, MNK derived neural stem cells (NSCs) were differentiated into neurons and astrocytes with 1 μ g of copper for 4 days (24). Concentration of copper ion in 1×10^6 MNK neurons and astrocytes was measured by ICP-MS. In MNK neurons and astrocytes, copper ion was accumulated in the cytoplasm approximately 20% more than wild type neurons and astrocytes (Supplementary Fig. S1B). This finding confirmed that excess copper in the MNK neurons and astrocytes is not efficiently eliminated due to ATP7A dysfunction.

Neurovascular abnormalities in the cerebral cortex and hippocampus of MNK mice

Copper accumulation could cause neurovascular abnormalities such as spiral angiogenesis in moyamoya disease (25). To examine whether the abnormal cerebral vascularization also occur in the MNK mice, we performed immunohistochemistry (IHC) and microCT analysis. Immunohistological staining of blood vessels reveals that the total number of GLUT+ blood vessels were significantly decreased in MNK cerebral cortex ($p=0.011$, Fig. 1A and 1B), but the number of blood vessels stained less than 25 μ m in length was increased in cerebral cortex of P14 MNK mice (Fig. 1B). Therefore, the proportion of the blood vessels stained less than 25 μ m was significantly increased in cerebral cortex of MNK mice (Fig. 1C). In addition, the sprouting formation of endothelial cells, which is usually observed during neovascularization, was dramatically reduced in the P14 MNK brain (Fig. 1A). Furthermore, brain vascular structures revealed by microCT images indicated that number of cerebral vessels was also severely decreased in the MNK brain (Fig. 1D). Interestingly, proportion of blood vessels stained less than 25 μ m in length was also significantly increased not only in the cerebral cortex, but also in the hippocampus in P13 MNK brains (Supplementary Fig. S2).

These neurovascular abnormalities in the MNK brain might affect development of NSCs in the hippocampal

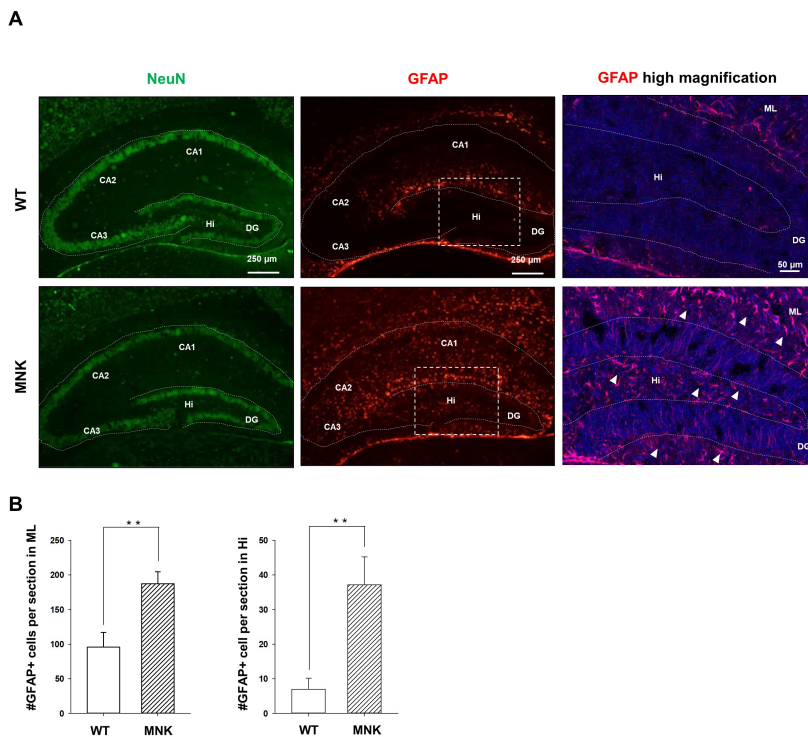


Fig. 3. Astrogenesis is promoted in the hippocampus of MNK mice. (A) Hippocampal sections were immunostained with neuronal marker NeuN and astrocyte marker GFAP at P13. The white box indicates regions shown in high magnification. DAPI was used to counterstain nuclei (Blue). (B) GFAP+ (Red, arrow-head) astrocytes in the highly magnified image were dramatically increased in the hilus and molecular layer of P13 of MNK mice compared with wild type. Scale bar 50 μ m and 250 μ m (high magnification). CA, Cornu ammonis; HI, Hilus; DG, dentate gyrus; ML, molecular layer. ** $p < 0.001$, $n = 4$ each, by t-test.

dentate gyrus. It is well known that vascularization of brain plays an important role in formation of NSC niche during postnatal development of CNS (26). In the DG of P13 MNK brains, NESTIN+ neural progenitor cells were significantly decreased, possibly due to the abnormal vascularization in the NSC niche (Fig. 1E). This finding showed that NSC Niche in the postnatal DG was severely compromised in MNK brain.

Reduced number of neural stem cells and their progeny is observed in the dentate gyrus of P13 MNK mice

To investigate NSC population in the DG of MNK mice, we examined NESTIN and SOX2 expressing cells. In the DG, NSCs express both NESTIN and SOX2 and extend their radial processes into the granule cell layer (GCL) from the subgranular zone (SGZ) (27). In the DG of P13 wild type mice, we observed NESTIN+, SOX2+

NSCs in SGZ and densely arranged radial NESTIN+ processes in GCL (Fig. 2A). In contrast, only very few NESTIN+, SOX2+ NSCs with these morphological characteristics were identified in the DG of P13 MNK mutant mice, suggesting abnormal formation of NSC population during postnatal development (Fig. 2A. arrowheads). In addition, the number of NESTIN+, SOX2+ NSCs was also dramatically decreased by 37% in the MNK SGZ compared to control (Fig. 2A).

Young neuroblasts originated from SGZ NSCs express doublecortin (DCX). While many DCX+ neuroblasts were observed in the DG of the wild type mice, almost no DCX+ neuroblasts were detected in the DG of MNK mice, consistent with very few SGZ NSCs and a lack of neurogenesis in MNK mice (Fig. 2A and 2B). The number of DCX+, PROX1+ neural progenitor cells were also significantly reduced by 65% in the GCL and SGZ of MNK mice compared to control (Fig. 2B). Furthermore, our IHC

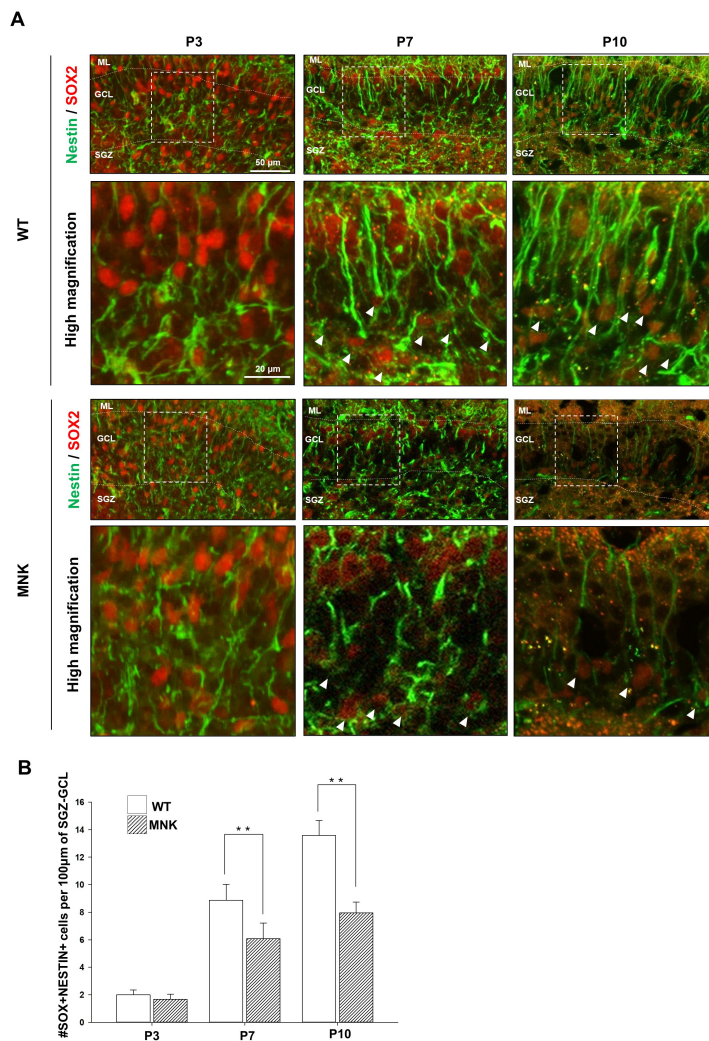


Fig. 4. Postnatal development of neural stem cell population in the dentate gyrus of MNK mice. (A) Dentate gyrus sections from MNK and wild type mice were stained with NESTIN and SOX2 during postnatal brain development (P3~P10). The white box indicates regions shown below (high magnification). Arrowheads indicate NESTIN+, SOX2+ neural stem cells. (B) Quantitative analysis of NESTIN+, SOX2+ cells during postnatal development of the DG. At P3, distribution of NESTIN+, SOX2+ cells in the dentate gyrus of MNK mice were not different from that of wild type. However, at P7 and P10, the number of NESTIN+, SOX2+ neural stem cells was significantly decreased in the SGZ of MNK mice. Scale bar 50 µm and 20 µm (high magnification). SGZ, subgranular zone; GCL, granule cell layer; ML, molecular layer. **p<0.001, n=4 each, by t-test.

data also support improper neuronal maturation in the DG of MNK mice (Fig. 2C). In wild type mice, NeuN+, Calbindin+ mature neurons were located in the upper part of GCL (Fig. 2C). In contrast, IHC revealed significant deficiency of NeuN+, Calbindin+ mature neurons in the DG of MNK mice. The number of NeuN+, Calbindin+ mature neurons was markedly decreased by 55% in the GCL of MNK mice compared to control (Fig. 2C). In addition, GFAP+ astrocytes were dramatically increased by 2-fold in the hilus and 5-fold in the CA region of the hippocampus in MNK mice compared to wild type (Fig. 3). These results suggest that insufficient neurogenesis and excess astrogenesis occur in the hippocampus of MNK mice.

Proper establishment of the postnatal NSC population is deficient in MNK mice

To investigate defects in postnatal development of the DG in MNK mice, establishment of the postnatal NSC population was examined with IHC from P3 to P10. DG in MNK mice was similar in size with wild type mice during postnatal brain development (P3~P14) (Supplementary Fig. S3). At P3, the number of NESTIN+, SOX2+ cells did not appear to be decreased in MNK mice (Fig. 4). At P7, NESTIN+, SOX2+ NSCs with radial processes started to appear in SGZ of wild type mice. However, ~36% fewer NESTIN+, SOX2+ NSCs with radial processes were observed in SGZ of MNK mice compared to wild type mice (Fig. 4). At P10, the number of NESTIN+, SOX2+ NSCs with radial processes were still decreased by ~31% in SGZ of MNK mice (Fig. 4). The decrease of postnatal NESTIN+, SOX2+ NSCs in MNK mice could result from increased cell death. However, activated Caspase3+ cells were not increased in the DG of P3, P7, and P10 MNK mice, suggesting that increased cell death was not responsible for the failure of the postnatal SGZ NSC expansion (Data not shown). Therefore, these results indicate that SGZ NSCs are not efficiently expanded during postnatal development in MNK mice.

Changes in cell proliferation could also affect the deficit of the SGZ NSCs in the DG of MNK mice. Overall, Ki67+ cells appeared to be decreased in the DG of P3~P10 MNK mice compared to controls (Fig. 5A). Interestingly, the number of SOX2+ progenitor cells expressing Ki67 in SGZ were also significantly reduced from P3 MNK mice (Fig. 5B). These results suggest that the proliferation of the SOX2+ progenitor cells was significantly compromised in the early postnatal MNK mice, indicating that the proper establishment of the postnatal NSC population during development was deficient in MNK mice.

Abnormal postnatal neurogenesis in DG of MNK mice

Granule neurons in DG are born mainly in early postnatal period with a peak of neurogenesis around P7 (28). However, in P7 brain of MNK mice, the SGZ NSC population already appeared deficient in number (Fig. 4).

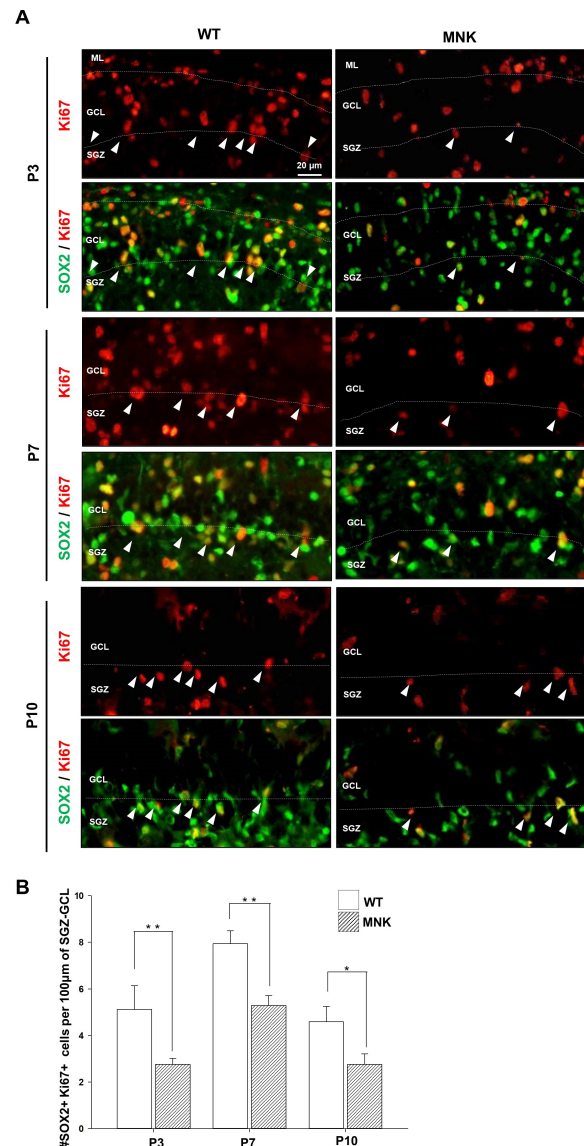


Fig. 5. Decrease of proliferating neural progenitor cells during DG development in MNK mice. (A) Dentate gyrus sections from MNK and wild type mice were stained with SOX2 and proliferation marker Ki67 during postnatal brain development (P3~P10). White arrowheads indicate SOX2+, Ki67+ proliferating neural progenitor cells. (B) Quantitative analysis of SOX2+, Ki67+ cells during postnatal development of the DG. SOX2+, Ki67+ proliferating neural progenitor cells in SGZ were significantly reduced in the MNK mice. Scale bar 20 μ m. SGZ, subgranular zone; GCL, granule cell layer; ML, molecular layer. * $p < 0.05$, ** $p < 0.001$, $n = 4$ each, by t-test.

Therefore, to investigate postnatal DG neurogenesis in MNK mice, DCX+ neuroblast population was examined from P3 to P10. As expected, DCX+ neuroblasts were not present yet in DG at P3, but at P7 DCX+ neuroblasts appeared in the upper GCL and hilus in wild type hippocampus (Fig. 6A). However, more than 40% of DCX+ neuroblasts were reduced at P7 and at P10 in the DG of MNK mice as compared to control (Fig. 6B). These results suggest that the failure of the SGZ NSC expansion may result in the deficiency in the postnatal neurogenesis in the DG of MNK mice.

Neurogenesis and neuronal maturation are severely compromised in MNK neurons *in vitro*

To further investigate neurogenesis from SGZ NSCs in MNK brain, *in vitro* neurosphere culture with SGZ NSCs was performed and neuronal differentiation was induced with media containing cytosine arabinoside (Ara C) (29). After 4 days of differentiation, neurospheres from control SGZ NSCs were spread on the bottom of a dish and neurite outgrowth from neurons derived from control SGZ NSCs was markedly increased (Fig. 7A). Neuronal differentiation potential of control SGZ NSCs was also decreased with neurosphere passaging (Fig. 7A). Interestingly, the number of MAP2+ neurons derived from MNK SGZ NSCs was dramatically decreased at each passage compared to that of control, and length and number of neurites was also significantly reduced by 59% and 15% respectively in MAP2+ neurons derived from P3 MNK SGZ NSCs compared to control (Fig. 7A). Moreover, western blot analysis also showed decrease of neurite specific proteins MAP2 in neurons from MNK mice throughout passage (Fig. 7B). These results indicate that neurogenesis and neuronal maturation are severely compromised in MNK neurons.

In addition to producing neurons, SGZ NSCs are able to generate astrocytes. Interestingly, expression of the astrocyte marker GFAP was significantly increased in the hippocampus of MNK mice (Fig. 3). To further investigate the developmental potential of SGZ NSCs, immunocytochemistry was performed with astrocytes derived from SGZ NSCs. Similar to our observation *in vivo*, MNK neurosphere cultures produced more GFAP+ astrocytes cells compared to wild type control (Fig. 7C). Furthermore, western blot analysis showed increased expression of active form of an astrogenesis specific transcription factor STAT3 (phosphorylated STAT3) and an astrogenic modulator JAK2 in the differentiated MNK NSCs (30) (Fig. 7D). In contrast, expression levels of a neurogenesis specific transcription factor NeuroD and neurogenic signal-

ing modulators ERK and pAKT were decreased in the differentiated MNK NSCs (31-33) (Fig. 7D). These results suggest increased astrogenesis instead of neurogenesis in MNK SGZ NSCs.

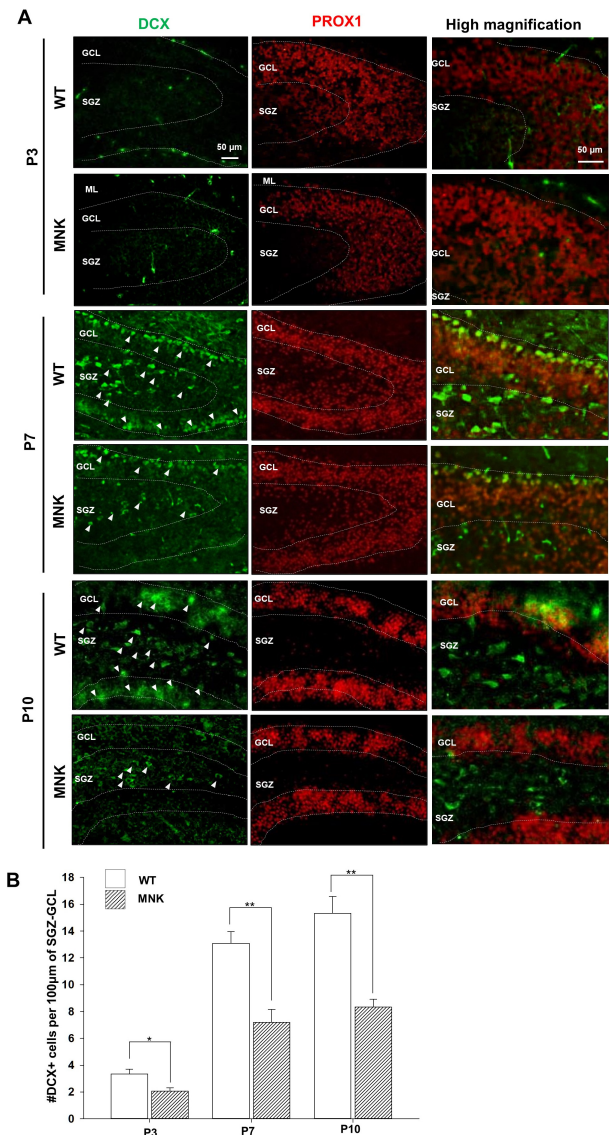


Fig. 6. Abnormal postnatal neurogenesis in the dentate gyrus of MNK mice. (A) Dentate gyrus sections from MNK and wild type mice were stained with neuroblast marker DCX and PROX1 during postnatal brain development (P3~P10). The number of DCX+ neuroblasts in the dentate gyrus of MNK mice was not different from that of wild type at P3. (B) Quantitative analysis of DCX+, PROX1+ cells during the postnatal development of the DG. More than 40% of DCX+ neuroblasts (arrowheads) were decreased at P7 and P10 in the DG of MNK mice. Scale bar 50 µm. SGZ, subgranular zone; GCL, granule cell layer; ML, molecular layer. * $p < 0.05$, ** $p < 0.001$, $n = 4$ each, by t-test.

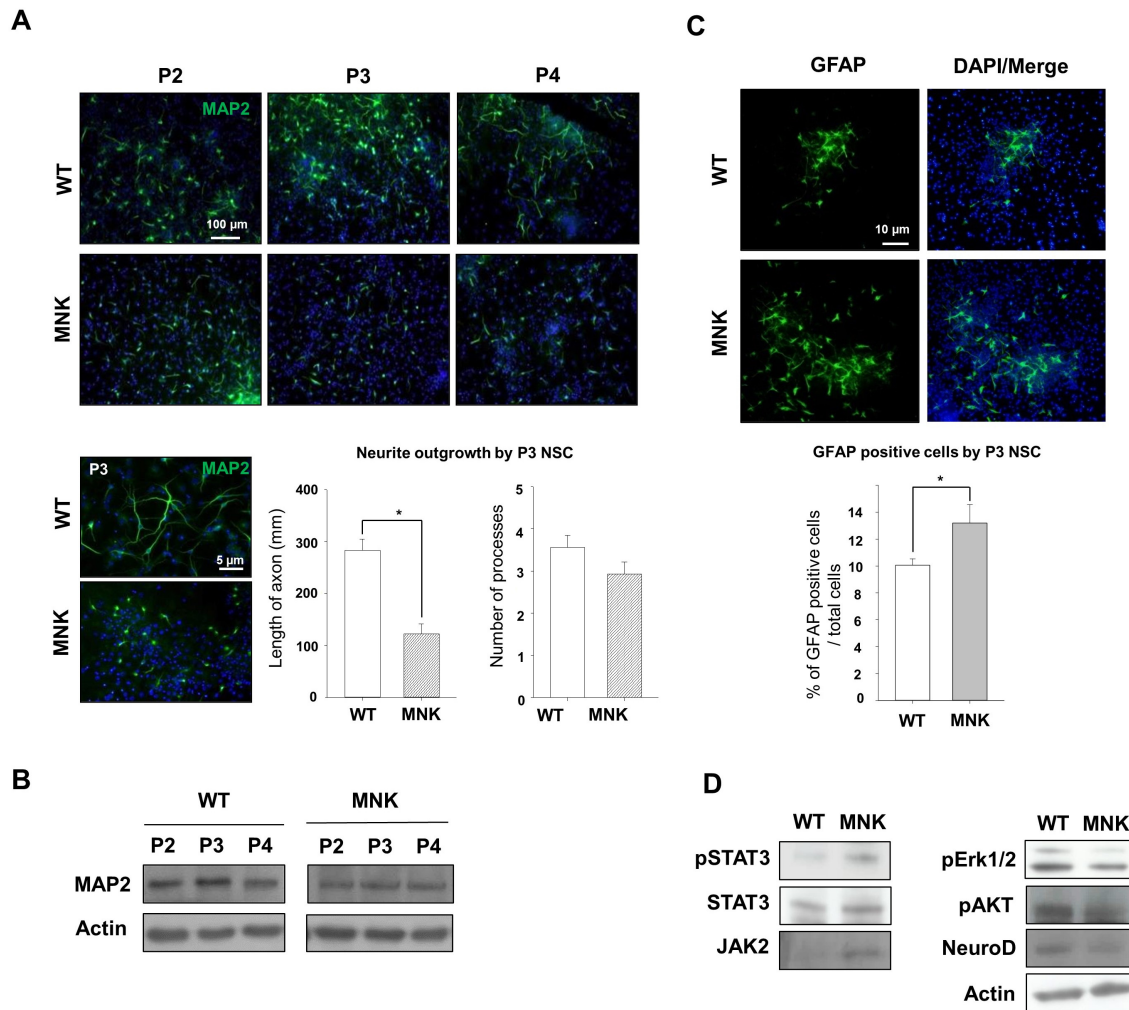


Fig. 7. Neurogenesis and neuronal maturation are severely compromised in MNK derived NSCs. Hippocampal neurosphere cultures from the brain of E18.5 wild type and MNK mice were established and induced neuronal differentiation for 4 days. (A) Neuronal processes marker MAP2 and DAPI (blue) were stained after neuronal differentiation. Neurite outgrowth of neurons derived from the hippocampal NSCs of MNK mice was significantly decreased through 4 passages in differentiation condition. Scale bar 100 μ m (upper), scale bar 5 μ m (lower). Metamorph analysis indicated more than 50% shorter neurites in the MNK derived neurons were observed relative to that of wild type. Scale bar 5 μ m. * $p < 0.05$ by t-test. (B) MAP2 expression was reduced in the MNK derived neurons compared with that of wild type through 4 passages. (C) Astrocyte marker GFAP+ cells were significantly increased in the MNK derived NSCs during neuronal differentiation. Scale bar 10 μ m. * $p < 0.05$ by t-test. (D) Western blot analysis was performed for neurogenesis makers (anti-NeuroD, anti-pAKT, and anti-pErk1/2) and astrogenesis makers (anti-pSTAT3 and anti-JAK2).

Discussion

Our study demonstrates that postnatal establishment of NSC population and their neurogenesis is severely compromised in the hippocampal DG of MNK mice, which plays a fundamental role in learning, memory, and behavior. In MNK mice, the number of neuroblasts and mature neurons was significantly reduced, which was related to loss of the SGZ NSC population and defective neuronal maturation (Fig. 2). To our knowledge, this is the first report demonstrating that insufficient expansion

of the postnatal NSC population may contribute to neurodevelopmental defects in MNK disease *in vivo*.

A variety of neurodegenerative symptoms occurs as a result of ATP7A dysfunction in MNK patients. Dysfunction of ATP7A leads to accumulation of copper in blood vessels and astrocytes, followed by deficiency of copper in neurons nearby, which eventually contribute to neurodegenerative symptoms in the CNS of MNK (22). Defects in the endothelial cells in blood vessels caused by abnormal accumulation of copper may induce cerebrovascular anomalies in MNK. In fact, abnormal elongation and tor-

tuous intracranial arteries and variation in wall thickness were previously reported in MNK patients (34). It has been also reported that excessive accumulation of copper may cause abnormal blood vessel formation or toxicity of endothelial cells (35). However, it has not been clear whether MNK mice also have the similar cerebrovascular defects. In this report, we observed that the number of major cerebral vessels and the total number of GLUT+ blood vessels was significantly decreased in the MNK mice (Fig. 1A, 1B, and 1D), while the proportion of blood vessels stained less than 25 μm in length was significantly increased in both cerebral cortex and hippocampus of P14 MNK mice (Fig. 1C and Supplementary Fig. S2). Due to the thin brain section (12 μm in thickness) and the optical depth of the fluorescence microscope used in this study, the significant decrease of the total number of the blood vessels but the significant increase of the proportion of the blood vessels stained less than 25 μm in length might reflect the existence of the tortuous vessels in the MNK brains. Therefore, further in-depth analysis of 3D vessel reconstruction with serial brain sections is required to confirm to the tortuous vascular structure in the MNK mice. These results suggest that mouse models of ATP7A dysfunction recapitulate brain defects of human MNK disease and may provide useful insight into pathology and therapies.

Neural development closely interacts with the vascular system at the beginning of the earliest stage of development, which persists throughout life (36). It has also been shown that vascular cells are key elements of the neural stem cell niches in the adult hippocampus and subventricular zone (26, 37). Therefore, we investigated whether abnormal hippocampal vascular structure in MNK mice can affect postnatal development of the NSC niche. In mice, SGZ NSC population is established during the early postnatal brain. After P7, NESTIN+, SOX2+ NSCs with radial processes and SOX2+, Ki67+ progenitor cells were significantly reduced in MNK mice compared to wild type control, suggesting that proper expansion of SGZ NSCs was failed during the postnatal development in MNK mice (Figs. 4 and 5). The reduction of the SGZ NSC population may lead to significant decrease of neuroblasts and mature neurons in the developing DG in MNK mice (Fig. 6). Interestingly, size of the developing DG in MNK mice was not reduced compared to wild type control during early postnatal period (P3~P14) (Supplementary Fig. S3). Meanwhile, GFAP+ astrocytes were significantly increased in the hippocampus of MNK mice (Fig. 3). Therefore, the size of DG may not be reduced in MNK mice because the increase of GFAP+

astrocytes could compensate the loss of neurons in the DG of MNK mice during the early postnatal development. These results suggest that abnormal establishment of NSCs in the brain contributes the early neurodegeneration and neurodevelopmental defects in MNK patients.

In addition to defects in establishment of postnatal NSCs, we also showed that neurogenesis from SGZ NSCs and neuronal maturation were severely compromised in MNK neurons (Fig. 7A and 7B). Since we isolated NSCs from E18.5 embryos and induced neurogenesis, our results suggest that copper deficiency may induce abnormal prenatal brain development in MNK disease. Moreover, increase in GFAP+ astrocytes was also observed in cerebral cortex and hippocampus in MNK mice (Fig. 3) and GFAP+ astrocytes differentiated from MNK SGZ NSCs were significantly increased *in vitro* (Fig. 7C and 7D). Interestingly, neuronal differentiation of MNK patient-derived induced pluripotent stem cells (iPSC) was also reduced (38). Copper itself is involved in the normal neuronal differentiation process. Copper chelation inhibited neurogenesis in P19 embryonic carcinoma cell lines (39). Copper was also required for neurite outgrowth in the rat pheochromocytoma PC-12 cells (40). Overall, these results support a prenatal onset of copper transfer related neurodevelopmental defects although MNK newborns appear neurologically normal.

Conclusions

Postnatal NSC niche is abnormally developed followed by severe defects of DG formation and loss of DG neurons in the MNK mouse model. Significant reduction of the postnatal neurogenesis in DG may contribute to neurodevelopmental symptoms in MNK. Our results provide new insights into the needs for new approaches in the therapeutic aspect of CNS damage in MNK patients.

Acknowledgments

This research was supported by a grant of the Korea Health Technology R&D Project through the Korea Health Industry Development Institute (KHIDI), funded by the Ministry of Health & Welfare, Republic of Korea (grant number : HI12C0066).

Potential Conflict of Interest

The authors have no conflicting financial interest.

Supplementary Materials

Supplementary data including three figures can be found

with this article online at <https://doi.org/10.15283/ijsc21088>.

References

- Vulpe C, Levinson B, Whitney S, Packman S, Gitschier J. Isolation of a candidate gene for Menkes disease and evidence that it encodes a copper-transporting ATPase. *Nat Genet* 1993;7:13 Erratum in: *Nat Genet* 1993;3:273
- Mercer JF, Livingston J, Hall B, Paynter JA, Begy C, Chandrasekharappa S, Lockhart P, Grimes A, Bhave M, Siemieniak D, Glover TW. Isolation of a partial candidate gene for Menkes disease by positional cloning. *Nat Genet* 1993;3:20-25
- Menkes JH, Alter M, Steigleder GK, Weakley DR, Sung JH. A sex-linked recessive disorder with retardation of growth, peculiar hair, and focal cerebral and cerebellar degeneration. *Pediatrics* 1962;29:764-779
- Kaler SG. ATP7A-related copper transport diseases-emerging concepts and future trends. *Nat Rev Neurol* 2011;7:15-29
- Paynter JA, Grimes A, Lockhart P, Mercer JF. Expression of the Menkes gene homologue in mouse tissues lack of effect of copper on the mRNA levels. *FEBS Lett* 1994;351:186-190
- Madsen E, Gitlin JD. Copper and iron disorders of the brain. *Annu Rev Neurosci* 2007;30:317-337
- Kodama H, Fujisawa C, Bhadhprasit W. Inherited copper transport disorders: biochemical mechanisms, diagnosis, and treatment. *Curr Drug Metab* 2012;13:237-250
- Qian Y, Tiffany-Castiglioni E, Welsh J, Harris ED. Copper efflux from murine microvascular cells requires expression of the menkes disease Cu-ATPase. *J Nutr* 1998;128:1276-1282
- Kaler SG, DiStasio AT. ATP7A-related copper transport disorders. In: Adam MP, Ardinger HH, Pagon RA, Wallace SE, Bean LJH, Gripp KW, Mirzaa GM, Amemiya A, editor. *GeneReviews*. Seattle: University of Washington; 1993.
- Donsante A, Yi L, Zerfas PM, Brinster LR, Sullivan P, Goldstein DS, Prohaska J, Centeno JA, Rushing E, Kaler SG. ATP7A gene addition to the choroid plexus results in long-term rescue of the lethal copper transport defect in a Menkes disease mouse model. *Mol Ther* 2011;19:2114-2123
- Deng W, Aimone JB, Gage FH. New neurons and new memories: how does adult hippocampal neurogenesis affect learning and memory? *Nat Rev Neurosci* 2010;11:339-350
- Ming GL, Song H. Adult neurogenesis in the mammalian brain: significant answers and significant questions. *Neuron* 2011;70:687-702
- Jacob FD, Habas PA, Kim K, Corbett-Detig J, Xu D, Studholme C, Glenn OA. Fetal hippocampal development: analysis by magnetic resonance imaging volumetry. *Pediatr Res* 2011;69(5 Pt 1):425-429
- Yu DX, Marchetto MC, Gage FH. How to make a hippocampal dentate gyrus granule neuron. *Development* 2014;141:2366-2375
- Wegiel J, Kuchna I, Nowicki K, Imaki H, Wegiel J, Marchi E, Ma SY, Chauhan A, Chauhan V, Bobrowicz TW, de Leon M, Louis LA, Cohen IL, London E, Brown WT, Wisniewski T. The neuropathology of autism: defects of neurogenesis and neuronal migration, and dysplastic changes. *Acta Neuropathol* 2010;119:755-770
- Mann JR, Camakaris J, Danks DM. Copper metabolism in mottled mouse mutants: distribution of ⁶⁴Cu in brindled (Mobr) mice. *Biochem J* 1979;180:613-619
- Emanuele P, Goodman ZD. A simple and rapid stain for copper in liver tissue. *Ann Diagn Pathol* 1998;2:125-126
- Weiss S, Dunne C, Hewson J, Wohl C, Wheatley M, Peterson AC, Reynolds BA. Multipotent CNS stem cells are present in the adult mammalian spinal cord and ventricular neuroaxis. *J Neurosci* 1996;16:7599-7609
- Ding Y, Zhang Z, Ma J, Xia H, Wang Y, Liu Y, Ma Q, Sun T, Liu J. Directed differentiation of postnatal hippocampal neural stem cells generates nuclear receptor related-1 protein- and tyrosine hydroxylase-expressing cells. *Mol Med Rep* 2016;14:1993-1999
- Wachs FP, Couillard-Despres S, Engelhardt M, Wilhelm D, Ploetz S, Vroemen M, Kaesbauer J, Uyanik G, Klucken J, Karl C, Tebbing J, Svendsen C, Weidner N, Kuhn HG, Winkler J, Aigner L. High efficacy of clonal growth and expansion of adult neural stem cells. *Lab Invest* 2003;83:949-962
- Doetsch F, Caillé I, Lim DA, García-Verdugo JM, Alvarez-Buylla A. Subventricular zone astrocytes are neural stem cells in the adult mammalian brain. *Cell* 1999;97:703-716
- Kodama H. Recent developments in Menkes disease. *J Inherit Metab Dis* 1993;16:791-799
- Tiffany-Castiglioni E, Qian Y. Astroglia as metal depots: molecular mechanisms for metal accumulation, storage and release. *Neurotoxicology* 2001;22:577-592
- Gonzalez-Perez O, Quiñones-Hinojosa A. Astrocytes as neural stem cells in the adult brain. *J Stem Cells* 2012;7:181-188
- Suzuki J, Takaku A. Cerebrovascular "moyamoya" disease. Disease showing abnormal net-like vessels in base of brain. *Arch Neurol* 1969;20:288-299
- Palmer TD, Willhoite AR, Gage FH. Vascular niche for adult hippocampal neurogenesis. *J Comp Neurol* 2000;425:479-494
- Patrício P, Mateus-Pinheiro A, Sousa N, Pinto L. Re-cycling paradigms: cell cycle regulation in adult hippocampal neurogenesis and implications for depression. *Mol Neurobiol* 2013;48:84-96
- Nicola Z, Fabel K, Kempermann G. Development of the adult neurogenic niche in the hippocampus of mice. *Front Neuroanat* 2015;9:53
- Negishi T, Ishii Y, Kyuwa S, Kuroda Y, Yoshikawa Y. Primary culture of cortical neurons, type-1 astrocytes, and microglial cells from cynomolgus monkey (*Macaca fascicularis*) fetuses. *J Neurosci Methods* 2003;131:133-140
- Rajan P, McKay RD. Multiple routes to astrocytic differ-

- entiation in the CNS. *J Neurosci* 1998;18:3620-3629
31. Rhim JH, Luo X, Gao D, Xu X, Zhou T, Li F, Wang P, Wong ST, Xia X. Cell type-dependent Erk-Akt pathway crosstalk regulates the proliferation of fetal neural progenitor cells. *Sci Rep* 2016;6:26547
 32. Peltier J, O'Neill A, Schaffer DV. PI3K/Akt and CREB regulate adult neural hippocampal progenitor proliferation and differentiation. *Dev Neurobiol* 2007;67:1348-1361
 33. Shioda N, Han F, Fukunaga K. Role of Akt and ERK signaling in the neurogenesis following brain ischemia. *Int Rev Neurobiol* 2009;85:375-387
 34. Cosimo QC, Daniela L, Elsa B, Carlo DV, Giuseppe F. Kinky hair, kinky vessels, and bladder diverticula in Menkes disease. *J Neuroimaging* 2011;21:e114-e116
 35. Kishimoto T, Fukuzawa Y, Abe M, Hashimoto M, Ohno M, Tada M. Injury to cultured human vascular endothelial cells by copper (CuSO₄). *Nihon Eiseigaku Zasshi* 1992;47:965-970
 36. Goldberg JS, Hirschi KK. Diverse roles of the vasculature within the neural stem cell niche. *Regen Med* 2009;4:879-897
 37. Shen Q, Temple S. Fine control: microRNA regulation of adult neurogenesis. *Nat Neurosci* 2009;12:369-370
 38. Suh JH, Kim D, Kim H, Helfman DM, Choi JH, Lee BH, Yoo HW, Han YM. Modeling of Menkes disease via human induced pluripotent stem cells. *Biochem Biophys Res Commun* 2014;444:311-318
 39. Watanabe M, Tezuka M. Copper is required for retinoic acid receptor-dependent transcription and neuronal differentiation in P19 embryonal carcinoma cells. *J Health Sci* 2006;52:540-548
 40. Birkaya B, Aletta JM. NGF promotes copper accumulation required for optimum neurite outgrowth and protein methylation. *J Neurobiol* 2005;63:49-61